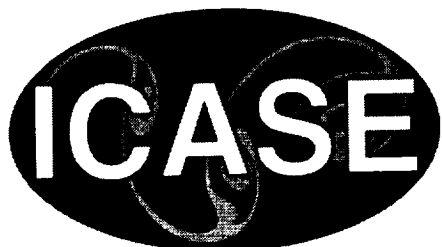


68115
NASA/CR-2002-211920
ICASE Report No. 2002-32



Differential Flatness and Cooperative Tracking in the Lorenz System

Luis G. Crespo
ICASE, Hampton, Virginia



October 2002

The NASA STI Program Office . . . in Profile

Since its founding, NASA has been dedicated to the advancement of aeronautics and space science. The NASA Scientific and Technical Information (STI) Program Office plays a key part in helping NASA maintain this important role.

The NASA STI Program Office is operated by Langley Research Center, the lead center for NASA's scientific and technical information. The NASA STI Program Office provides access to the NASA STI Database, the largest collection of aeronautical and space science STI in the world. The Program Office is also NASA's institutional mechanism for disseminating the results of its research and development activities. These results are published by NASA in the NASA STI Report Series, which includes the following report types:

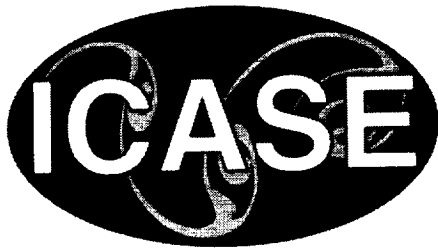
- **TECHNICAL PUBLICATION.** Reports of completed research or a major significant phase of research that present the results of NASA programs and include extensive data or theoretical analysis. Includes compilations of significant scientific and technical data and information deemed to be of continuing reference value. NASA's counterpart of peer-reviewed formal professional papers, but having less stringent limitations on manuscript length and extent of graphic presentations.
- **TECHNICAL MEMORANDUM.** Scientific and technical findings that are preliminary or of specialized interest, e.g., quick release reports, working papers, and bibliographies that contain minimal annotation. Does not contain extensive analysis.
- **CONTRACTOR REPORT.** Scientific and technical findings by NASA-sponsored contractors and grantees.
- **CONFERENCE PUBLICATIONS.** Collected papers from scientific and technical conferences, symposia, seminars, or other meetings sponsored or cosponsored by NASA.
- **SPECIAL PUBLICATION.** Scientific, technical, or historical information from NASA programs, projects, and missions, often concerned with subjects having substantial public interest.
- **TECHNICAL TRANSLATION.** English-language translations of foreign scientific and technical material pertinent to NASA's mission.

Specialized services that complement the STI Program Office's diverse offerings include creating custom thesauri, building customized data bases, organizing and publishing research results . . . even providing videos.

For more information about the NASA STI Program Office, see the following:

- Access the NASA STI Program Home Page at <http://www.sti.nasa.gov>
- Email your question via the Internet to help@sti.nasa.gov
- Fax your question to the NASA STI Help Desk at (301) 621-0134
- Telephone the NASA STI Help Desk at (301) 621-0390
- Write to:
NASA STI Help Desk
NASA Center for AeroSpace Information
7121 Standard Drive
Hanover, MD 21076-1320

NASA/CR-2002-211920
ICASE Report No. 2002-32



Differential Flatness and Cooperative Tracking in the Lorenz System

Luis G. Crespo
ICASE, Hampton, Virginia

ICASE
NASA Langley Research Center
Hampton, Virginia

Operated by Universities Space Research Association



Prepared for Langley Research Center
under Contract NAS1-97046

October 2002

Available from the following:

NASA Center for AeroSpace Information (CASI)
7121 Standard Drive
Hanover, MD 21076-1320
(301) 621-0390

National Technical Information Service (NTIS)
5285 Port Royal Road
Springfield, VA 22161-2171
(703) 487-4650

DIFFERENTIAL FLATNESS AND COOPERATIVE TRACKING IN THE LORENZ SYSTEM*

LUIS G. CRESPO†

Abstract. In this paper the control of the Lorenz system for both stabilization and tracking problems is studied via feedback linearization and differential flatness. By using the Rayleigh number as the control -only variable physically tunable- a barrier in the controllability of the system is incidentally imposed. This is reflected in the appearance of a singularity in the state transformation. Composite controllers that overcome this difficulty are designed and evaluated. The transition through the manifold defined by such a singularity is achieved by inducing a chaotic response within a boundary layer that contains it. Outside this region, a conventional feedback nonlinear control is applied. In this fashion, the authority of the control is enlarged to the whole state space and the need for high control efforts is mitigated. In addition, the differential parametrization of the problem is used to track nonlinear functions of one state variable (single tracking) as well as several state variables (cooperative tracking). Control tasks that lead to integrable and non-integrable differential equations for the nominal flat output in steady-state are considered. In particular, a novel numerical strategy to deal with the non-integrable case is proposed. Numerical results validate very well the control design.

Key words. feedback linearization, differential flatness, Lorenz system, cooperative tracking, non-linear control

Subject classification. Applied and Numerical Mathematics

1. Introduction. The analysis and control of chaotic systems have attracted considerable attention in recent years. A chaotic system is strongly sensitive to small changes in the initial conditions. Such a behavior can be beneficial or detrimental depending upon the system and the objective under investigation. In this paper we will make use of the chaotic response of the Lorenz system to enhance the performance and controllability of feedback linearization based controllers.

The Lorenz system is a simplified model of a thermally driven fluid convection system between parallel plates. Depending on the system parameters, such a system exhibits a rich spectrum of responses. The control of the Lorenz system has been studied by several researchers in recent years. Vincent and Yu [10] proposed a bang-bang optimal control for stabilizing the unstable equilibrium points of the system. Gao and colleagues [5] studied the nonlinear feedback control based on state space design. Chen and Liu [2], Talwar and Namachchivaya [9] and Alvarez-Gallegos [1] investigated the nonlinear regulation of the Lorenz system by using the feedback linearization techniques with different control structures and control objectives.

From the physics point of view, it is natural to select the Rayleigh number as the control variable. However, such a strategy makes the system uncontrollable at the plane $x = 0$. This control variable was used by the author in [3]. When feedback linearization techniques are applied, this feature appears as a singularity in the state transformation. When the feedback linearization techniques are applied, this feature also appears as a singularity in the state transformation. The controllability of the system is limited to half of the state space. The singularity is also responsible for extremely high control efforts in its vicinity. In this

*This work was supported by the National Aeronautics and Space Administration under NASA Contract No. NAS1-97046 while the author was in residence at ICASE, NASA Langley Research Center

†ICASE, Mail Stop 132C, NASA Langley Research Center, Hampton, VA 23681-2199, USA, e-mail: lgcrespo@icase.edu.

paper, we propose composite controllers to overcome this limitation. Within a boundary layer that contains such a singularity, the chaotic response of the system and its response to step inputs are used to drive the system through. Furthermore, the differential flatness of the system is used to aim for control objectives that do and do not admit a closed form expression for the corresponding flat output of the system.

This paper is organized as follows. A brief description and analysis of the Lorenz system are presented in Section 2. Section 3 discusses the feedback linearization and its application to the Lorenz system. In Section 4, composite controllers are designed and evaluated for both stabilization and tracking problems.

2. The Lorenz System. The Lorenz model is obtained from studying a fluid layer heated from below and cooled from above such that a temperature difference is established across it. The convection motion is described by the Navier-Stokes equations. Taking Fourier expansion of these equations along two spatial directions and truncating the remaining expressions to retain only three modes leads to the following simplified model

$$\begin{aligned}\dot{x} &= \sigma(y - x), \\ \dot{y} &= \rho x - y - xz, \\ \dot{z} &= -\beta z + xy,\end{aligned}\tag{2.1}$$

where σ , ρ and β are real parameters denoting the Prandtl number, the Rayleigh number and a geometric factor, respectively. The state variables x , y and z represent measures of fluid velocities and the spatial temperature distribution in the fluid layer under gravity. From the physical point of view, the Rayleigh number ρ can be easily manipulated by changing the heat transfer to the fluid from below. This parameter will be treated as the control variable. We denote $u \equiv \rho$.

For the brevity of discussion, we assume that the control converges to a constant value in steady state denoted as $u_{ss} \equiv \lim_{t \rightarrow \infty} u$. The singular points of the system can be parametrized with u_{ss} . The locus of these points is given by a family of curves

$$X_1^* = [0, 0, 0]^T, \quad X_{2,3}^* = [\pm\sqrt{\beta(u_{ss} - 1)}, \pm\sqrt{\beta(u_{ss} - 1)}, u_{ss} - 1]^T.\tag{2.2}$$

Linearization about X_1^* leads to characteristic equation $\lambda^3 + A\lambda^2 + B\lambda + C = 0$, where $A = 1 + \beta + \sigma$, $B = \beta(\sigma + 1) + \sigma - u_{ss}$ and $C = \beta(\sigma - u_{ss})$. Linearization about $X_{2,3}^*$ leads to $A = 1 + \beta + \sigma$, $B = \beta(u_{ss} + \sigma)$ and $C = 2\beta\sigma(u_{ss} - 1)$.

The stability analysis leads to the following observations. When $u_{ss} < 1$ the origin of the system is a stable equilibrium point. When $1 < u_{ss} < \hat{\rho} \equiv \sigma(\sigma + \beta + 3)/(\sigma - \beta - 1)$, X_1^* is unstable and $X_{2,3}^*$ are stable. When $u_{ss} > \hat{\rho}$ there are no stable equilibrium points and the system reaches a chaotic regime.

At $u_{ss} = 1$ a pitchfork bifurcation takes place at X_1^* , while for $u_{ss} = \hat{\rho}$ a subcritical Hopf bifurcation occurs at $X_{2,3}^*$. For $u_{ss} \geq \hat{\rho}$, the system is driven by repulsions exclusively while the trajectories are confined to a region of finite volume forming a strange attractor. The response on the attractor is chaotic. For additional information, the reader can refer to [8]. In the numerical simulations, the parameters to be used are $\sigma = 10$ and $\beta = 8/3$.

3. Feedback State Linearization.

3.1. Background. Consider the single input system

$$\dot{\mathbf{x}} = \mathbf{f}(\mathbf{x}) + \mathbf{g}(\mathbf{x})u,\tag{3.1}$$

where $\mathbf{x} \in \mathbf{R}^n$ is the state vector, $u \in \mathbf{R}$ is the control and $\mathbf{f}, \mathbf{g} : \mathbf{R}^n \rightarrow \mathbf{R}^n$ are sufficiently smooth nonlinear functions of their arguments. The Lie derivative of $\mathbf{g}(\mathbf{x})$ with respect to the vector field $\mathbf{f}(\mathbf{x})$ is defined as

$$\begin{aligned} ad_{\mathbf{f}}^k \mathbf{g}(\mathbf{x}) &= [\mathbf{f}, ad_{\mathbf{f}}^{k-1} \mathbf{g}](\mathbf{x}) \text{ for } k \geq 1, \\ ad_{\mathbf{f}}^0 \mathbf{g}(\mathbf{x}) &= \mathbf{g}(\mathbf{x}), \end{aligned} \quad (3.2)$$

where $[\mathbf{X}, \mathbf{Y}] = \nabla \mathbf{Y} \cdot \mathbf{X} - \nabla \mathbf{X} \cdot \mathbf{Y}$ is the Lie bracket of the vector fields \mathbf{X} and \mathbf{Y} . According to [6], there exists a real value function $\lambda(\mathbf{x})$, defined in a neighborhood $U(\mathbf{x}_0)$ of \mathbf{x}_0 such that

$$\begin{aligned} L_{\mathbf{g}} \lambda(\mathbf{x}) &= L_{ad_{\mathbf{f}} \mathbf{g}} \lambda(\mathbf{x}) = \dots = L_{ad_{\mathbf{f}}^{n-2} \mathbf{g}} \lambda(\mathbf{x}) = 0, \\ L_{ad_{\mathbf{f}}^{n-1} \mathbf{g}} \lambda(\mathbf{x}_0) &\neq 0, \end{aligned} \quad (3.3)$$

where $L_{\mathbf{g}} \lambda(\mathbf{x}) = \nabla \lambda(\mathbf{x}) \cdot \mathbf{g}$ denotes the Lie derivative of the real-value function $\lambda(\mathbf{x})$ with respect to the vector field \mathbf{g} , if (i) the matrix

$$\mathbf{C} = [\mathbf{g}(\mathbf{x}_0), ad_{\mathbf{f}} \mathbf{g}(\mathbf{x}_0), ad_{\mathbf{f}}^2 \mathbf{g}(\mathbf{x}_0), \dots, ad_{\mathbf{f}}^{n-1} \mathbf{g}(\mathbf{x}_0)], \quad (3.4)$$

has rank n and (ii) the distribution $D = \text{span}\{\mathbf{g}(\mathbf{x}), ad_{\mathbf{f}} \mathbf{g}(\mathbf{x}), ad_{\mathbf{f}}^2 \mathbf{g}(\mathbf{x}), \dots, ad_{\mathbf{f}}^{n-1} \mathbf{g}(\mathbf{x})\}$ is involutive. Furthermore, there exists a transformation $\mathbf{z} = \Phi(\mathbf{x})$ in $U(\mathbf{x}_0)$ such that

$$\begin{aligned} \Phi(\mathbf{x}) &= [\lambda(\mathbf{x}), L_{\mathbf{f}} \lambda(\mathbf{x}), \dots, L_{\mathbf{f}}^{n-1} \lambda(\mathbf{x})]^T, \\ &= [\lambda(\mathbf{x}), \dot{\lambda}(\mathbf{x}), \dots, \frac{d^{n-1} \lambda(\mathbf{x})}{dt^{n-1}}]^T. \end{aligned} \quad (3.5)$$

The system (3.1) is transformed into a chain of integrators

$$\dot{z}_1 = z_2, \dot{z}_2 = z_3, \dots, \dot{z}_{n-1} = z_n, \dot{z}_n = a(\mathbf{x}) + b(\mathbf{x})u \equiv v, \quad (3.6)$$

$$v(\mathbf{x}) = a(\mathbf{x}) + b(\mathbf{x})u = L_{\mathbf{g}} L_{\mathbf{f}}^{n-1} \lambda(\mathbf{x}) + L_{\mathbf{f}}^n \lambda(\mathbf{x})u, \quad (3.7)$$

where $z_i = L_{\mathbf{f}}^{i-1} \lambda(\mathbf{x})$ ($i = 1, \dots, n$). The control for this linear system can be designed by full state feedback and pole placement techniques. For example, the control v can be taken as:

$$v(\Phi^{-1}(\mathbf{z})) = -\mathbf{K}\mathbf{z}, \quad (3.8)$$

where the feedback gains \mathbf{K} are chosen to place the closed loop poles at the desired locations in the left hand side of the complex plane. For tracking problems, the feedback signal will be the tracking error $\mathbf{z}_d - \mathbf{z}$ where \mathbf{z}_d is a pre-specified reference signal in the \mathbf{z} -domain.

The control in the physical domain is then given by:

$$u(\mathbf{x}) = [v(\Phi^{-1}(\mathbf{z})) - a(\mathbf{x})] / b(\mathbf{x}). \quad (3.9)$$

It should be noted that $u(\mathbf{x})$ becomes unbounded when $b(\mathbf{x}) \rightarrow 0$.

3.2. Feedback Linearization of the Lorenz System. For the Lorenz system, $\mathbf{f} = [\sigma(y - x), -y - xz, -\beta z + xy]^T$ and $\mathbf{g} = [0, x, 0]^T$. After some manipulations we obtain

$$\begin{aligned} ad_{\mathbf{g}}(ad_{\mathbf{f}} \mathbf{g}) &= [0, 2\sigma x, 0]^T, \\ ad_{\mathbf{f}} \mathbf{g} &= [-\sigma x, \sigma(y - x) + x, -x^2]^T, \\ ad_{\mathbf{f}}^2 \mathbf{g} &= \begin{bmatrix} \sigma(\sigma - 1)x - 2\sigma^2 y \\ -x^3 - 2\sigma xy + (\sigma - 1)^2 x + \sigma(1 - \sigma)y \\ (3\sigma - 1 - \beta)x^2 - 2\sigma xy \end{bmatrix}. \end{aligned} \quad (3.10)$$

By evaluating the rank of the \mathbf{C} matrix in Equation (3.4), we find that the rank is 3 except when the transformation is singular at $x = 0$ or $\sigma = \beta/2$. At the singularity at $x = 0$, the system (2.1) is completely insensitive to the control. This restriction imposes an unavoidable barrier in the controllability of the system, leaving just half of the state space at the disposal of the control. Which half the system stays in depends on the initial condition. The closer the system gets to this singular plane, the higher the control effort will be, approaching positive or negative infinity as x approaches to zero.

From Equation (3.3), the function $\lambda(\mathbf{x})$, known as the flat output of the system [4, 7], satisfies

$$\begin{aligned} x \frac{\partial \lambda}{\partial y} &= 0, \\ -\sigma x \frac{\partial \lambda}{\partial x} + ((1 - \sigma)x + \sigma) \frac{\partial \lambda}{\partial y} - x^2 \frac{\partial \lambda}{\partial z} &= 0. \end{aligned} \quad (3.11)$$

Solving this set of equations, we obtain $\lambda = x^2/2 - \sigma z + k$, where k is the integration constant. Equation (3.5) leads to the state transformation

$$\begin{aligned} \mathbf{z} &= [z_1, z_2, z_3]^T \equiv \Phi(\mathbf{x}) \\ &= [x^2/2 - \sigma z + k, \sigma(\beta z - x^2), \sigma \gamma xy + 2\sigma^2 x^2 - \sigma \beta^2 z]^T, \end{aligned} \quad (3.12)$$

where $\gamma \equiv \beta - 2\sigma$. The inverse transformation is given by

$$\begin{aligned} \mathbf{x} &= [x, y, z]^T \equiv \Phi^{-1}(\mathbf{z}) \\ &= \left[\pm \sqrt{\frac{2(\beta \varepsilon + z_2)}{\gamma}}, \pm \frac{2\sigma \beta z_1 + (\beta + 2\sigma)z_2 + z_3 - 2\sigma \beta k}{\sigma \sqrt{2\gamma(\beta \varepsilon + z_2)}}, \frac{2\sigma \varepsilon + z_2}{\sigma \gamma} \right]^T, \end{aligned} \quad (3.13)$$

where $\varepsilon \equiv z_1 - k$. The transformed dynamic system takes the form of Equation (3.6) with $n = 3$ and $a(\mathbf{x})$ and $b(\mathbf{x})$ in Equation (3.7) given by

$$\begin{aligned} a(\mathbf{x}) &= -\sigma \gamma x^2 z - 4\sigma^3 x^2 - \sigma(\gamma + \beta^2 + \sigma\beta - 6\sigma^2)xy + \sigma^2 \gamma y^2 + \sigma \beta^3 z, \\ b(\mathbf{x}) &= \sigma \gamma x^2. \end{aligned} \quad (3.14)$$

By using the solution of the PDE (3.11) and the system equation (2.1), we have

$$\begin{aligned} \lambda &= x^2/2 - \sigma z + k, \\ \dot{\lambda} &= \sigma(\beta z - x^2), \\ \ddot{\lambda} &= \sigma \gamma xy + 2\sigma^2 x^2 - \beta^2 \sigma z. \end{aligned} \quad (3.15)$$

The state variables and the control can be differentially parametrized using the flat output.

$$\begin{aligned} x &= \pm \sqrt{2\kappa/\gamma}, \\ y &= \pm(\ddot{\lambda} + (\beta + 2\sigma)\dot{\lambda} + 2\sigma\beta\lambda - 2\sigma k)/(\sigma\sqrt{2\gamma\kappa}), \\ z &= (\beta\dot{\lambda} + 2\sigma\beta\lambda - 2\sigma k)/(\sigma\beta\gamma), \\ u &= \frac{1}{4\sigma\beta\gamma\kappa^2} \{ -2\beta\gamma\kappa v - 2\beta\gamma(\beta\kappa + \kappa + 2c\sigma - \sigma k)\ddot{\lambda} - 2\beta(4kc - 2c^2 - 2k^2 + 2\sigma\gamma\kappa + \\ &\quad \beta\gamma\kappa + 2\sigma\beta\gamma c - \gamma\sigma\beta k)\dot{\lambda} - 4\sigma\beta(\beta\gamma\kappa + 4kc - 2c^2 - 2k^2)\lambda - 8\sigma k c^2 + 4\sigma\beta\gamma k \kappa - 8\sigma k^3 + \\ &\quad 16\sigma k^2 c + \beta^2 \gamma(\beta + 2\sigma)\dot{\lambda}^2 + 2\beta\gamma(\beta + \sigma)\ddot{\lambda}\dot{\lambda} + \beta\gamma\ddot{\lambda}^2 + 2\sigma\beta^2 \gamma\ddot{\lambda}\lambda + 2\sigma\beta^3 \gamma\dot{\lambda}\lambda \}, \end{aligned} \quad (3.16)$$

where $c \equiv \dot{\lambda} + \beta\lambda$, $\kappa \equiv c - k$ and $v \equiv \ddot{\lambda}$. Inequality range constraints on u can be imposed by designing composite controllers. This is explained in the next section.

4. Composite Control. From the above discussions, we know that a feedback linearization based control is not able to drive the system across the singularity imposed by the transformation. This fact restricts the controllability of the system to a portion of the state space, half in this case, and leads to extremely high control effort in the vicinity of the singularity. In this section we propose a composite controller to overcome such a difficulty.

Denote the hyper-plane that makes the state transformation singular as $g(\mathbf{x}) = 0$. Define the composite controller given by:

$$u(\mathbf{x}) = \begin{cases} u_1 & \text{if } |\mathbf{x} - g(\mathbf{x})| > \delta \\ u_2 & \text{otherwise} \end{cases} \quad (4.1)$$

where δ defines the thickness of a boundary layer about the singular plane, u_1 is the control expression resulting from using a conventional control method and u_2 is the amplitude of a step input set according to the particular control objectives.

The condition for applying u_1 can be replaced by $|u_1| < U$, provided that control saturation occurs in the vicinity of the boundary layer. In this paper, $g(\mathbf{x}) = 0$ and u_2 is a step input that induces a chaotic response within the boundary layer i.e. $u_2 > \hat{\rho}$.

The non-empty intersection of the attractor and the two hyper-planes defined by $|\mathbf{x} - g(\mathbf{x})| = \delta$ guarantees that the crossing of the boundary layer occurs. This can be proved as follows. Let's call $h_i(\mathbf{x})$ for $i = 1, 2$ these two planes. Assume that (i) the chaotic response is moving within a strange attractor whose state space location is given by A_1 and that (ii) $A_1 \cap h_i(\mathbf{x}) \neq \emptyset$. The crossing of the hyper-plane $h_i(\mathbf{x})$ will not occur iff there exist a subset $A_2 \subset A_1$ such that $A_2 \cap h_i(\mathbf{x}) = \emptyset$ for all times i.e. A_2 is a strange attractor by itself. This implication violates the irreducibility property of A_1 then A_2 can not exist. The need for $A_1 \cap h_i(\mathbf{x}) \neq \emptyset$ imposes bounds to δ from above.

Notice that in this scheme the control does not have the authority to manipulate the transient part of the transition from one side of the boundary layer to the other one. For some states several crossings of $g(\mathbf{x})$ might occur before the system leaves the boundary layer. Such behavior is clearly undesirable. Refinements and improvements of the control within the boundary layer can be achieved by taking into consideration the control objective and the state of the system. This practice however was not implemented in this study. Once the system leaves the boundary layer u_1 is applied and the stabilization/tracking is achieved. In this paper u_1 is given by u in Equation (3.16). Due to the structure of the controller, global uniform asymptotic stability about the reference signal $r(\mathbf{x}(t))$ is achieved at the locations where the intersection of $r(\mathbf{x}(t))$ and the boundary layer is an empty set.

For stabilization, the linear system given by Equations (3.6), (3.7) and (3.14) can be controlled by pole placement techniques. Taking the feedback control v as:

$$v = \alpha_1 z_1 + \alpha_2 z_2 + \alpha_3 z_3, \quad (4.2)$$

where the feedback gains α_i are chosen to place the closed loop poles in the left hand side of the complex plane. On the original state variables, the control can be obtained after substituting Equations (3.12) and (3.8) into Equation (3.7). Since this procedure stabilizes \mathbf{z} , the steady-state values in the x -domain can be controlled by manipulating k according to Equation (3.13). The reader must notice that stabilization about the origin using feedback linearization requires infinite control effort, i.e. $\lim_{x \rightarrow 0} u(\mathbf{x}) = \lim_{x \rightarrow 0} (v(\mathbf{x}) - a(\mathbf{x}))/b(\mathbf{x}) = \pm\infty$. However, from the stability analysis we know that any control satisfying $0 < u_{ss} < 1$ will drive the system to the origin from a given initial condition.

4.1. Single State Tracking Control. In this section we present examples for stabilization and tracking control problems that involve a single state. The tracking signal $x_d(t) = a + b\sin(t)$ for the state variable $x(t)$ is considered here. The flat output corresponding to the tracking signal $x_d(t)$ is given by

$$\begin{aligned}\lambda_d(t) = & (\gamma/2\beta)(b^2/2 + a^2) + (\gamma ab/(\beta^2 + 1)) \{\beta \sin(t) - \cos(t)\} \\ & - (b^2\gamma/(2\beta^2 + 8))\{(\beta/2) \cos(2t) - \sin(2t)\}\end{aligned}\quad (4.3)$$

The difference between the system flat output, $\lambda_d - \lambda = z_d - z_1$ is the tracking error. We take the full state feedback control v for the tracking problem as follows

$$v = \ddot{\lambda}_d + K_1(\ddot{\lambda}_d - \ddot{\lambda}) + K_2(\dot{\lambda}_d - \dot{\lambda}) + K_3(\lambda_d - \lambda) \quad (4.4)$$

The control gains K_i are selected such that the tracking error vanishes exponentially. It should be noted that the tracking control is designed in the transformed space \mathbf{z} , and therefore is indirect for \mathbf{x} .

The state variables and the nominal control obtained from Equation (3.16) are shown in Figure 5.1 for $a = 5$ and $b = 6$. The control grows unbounded near the singularity. Time evolutions for different $x_d(t)$ are shown in Figures 5.2 and 5.3 using $\delta = 0.1$ and $\delta = 0.2$ respectively. In all the cases the control is activated after 30 seconds of chaotic regime. In the first case, the system does not reach the boundary layer and perfect tracking is achieved after a short transient. If the control is activated when the singular plane is between the state of the system and $x_d(t)$, the system would reach and cross the boundary layer before settling down. This control was designed such that u_2 is applied when $u_1 < \delta$. In this fashion the control range constraint $u > 0$ is imposed. In the second case, the desired trajectory crosses repeatedly the singular plane forcing the system to reach the boundary layer several times. The effect of not applying the nominal control is slightly noticeable. The reader must notice that both the x and y states behave similarly once the system reaches the strange attractor.

Figure 5.4 shows the results of the composite controller with a wider boundary layer $\delta = 0.5$. Recall that the control does not have authority within the boundary layer and relies on the chaotic behavior of the system to cross it. As expected, the increase of δ has a detrimental effect on the control performance. For even higher values of δ , the system might be trapped in the boundary layer while the desired trajectory completes half a cycle.

4.2. Cooperative Tracking Control. Now we use the differential parametrization of the states and control to aim for tracking objectives that involve combinations of the states. The problem statement is as follows. Find u_1 in Equation (4.1) such that the system is driven to the manifold defined by $h(\mathbf{x}, u, t) = 0$ from any initial condition. In this problem, the system would track signals that imply cooperative relations among the states, being the tracking of a trajectory of a particular state a particular case. Again, the composite structure of the control enable to achieve global stability about the desired tracking function. In the examples to come we will take $u_2 = 30 > \hat{\rho}$ within the boundary layer.

Depending upon the tracking objective, the equation for the desired flat output can be integrable or non-integrable. Both cases are considered next.

4.2.1. Problems with closed form solution for λ_d . Once the control objective $h(\mathbf{x}, u, t) = 0$ is set, the Equations (3.16) lead to an ODE for the desired flat output λ_d . Such an equation is in general non-linear. In this section we study problems where a closed form expression for the steady state solution can be found.

As the first example, we take $h(\mathbf{x}, u, t) = x^2 - z - a - b\sin(\omega t)$. The corresponding differential equation for the flat output is given by

$$\dot{\lambda}_d + (2\sigma\xi/\phi)\lambda_d = a\sigma\gamma/\phi + (b\sigma\gamma/\phi)\sin(\omega t),$$

where $\phi \equiv 2\sigma - 1$ and $\xi \equiv \beta - 1$. Solving we find

$$\lambda_d = a\gamma/(2\xi) + \eta \exp\{-2t\sigma\xi/\phi\} + \{2b\sigma^2\gamma\xi \sin(\omega t) - \omega b\sigma\gamma\phi \cos(\omega t)\}/(4\sigma^2\xi^2 + \omega^2\phi^2). \quad (4.5)$$

For our purposes, providing that the transient response vanishes, only the steady state component is needed. This expression along with Equations (3.16) and (4.4) fully determine the control. After some manipulations we find that the system reaches stationarity at

$$\begin{aligned} \mathbf{x}_{ss} &= \left[\mp \sqrt{\beta a/\xi}, \mp \sqrt{\beta a/\xi}, a/\xi \right]^T, \\ u_{ss} &= 2 + (a - \xi)/\xi, \end{aligned} \quad (4.6)$$

Numerical results for $a = 15$ and $b = 5$ are shown in Figure 5.5. For this particular case, the system crosses the boundary layer twice. Figure 5.6 shows the numerical results for $a = 10$ and $b = 0$.

As a second case, we use $h(\mathbf{x}) = x^2 + y^2 + z^2 - R^2$. This problem can be interpreted as the stabilization of the system about the surface of a sphere. The corresponding differential equation for λ_d , not shown here, is non-linear. However, because the homogeneous solution vanishes with time we can solve for particular solution and use it in Equation (4.4) to calculate the control. The corresponding flat output and steady state values are:

$$\begin{aligned} \lambda_d &= \gamma(\pm\theta - \beta)/2, \\ \mathbf{x}_{ss} &= \left[\pm\sqrt{\beta(\theta - \beta)}, \pm\sqrt{\beta(\theta - \beta)}, \theta - \beta \right]^T, \\ u_{ss} &= \pm(1 + \theta - \beta), \end{aligned}$$

where $\theta = \sqrt{\beta^2 + R^2}$. Stationary values of the states can also be found by solving for the values of k in Equation (3.13) that satisfy $h(\mathbf{x}) = 0$ when $\mathbf{z} \rightarrow 0$ (due to Equation (3.8)). Numerical results for $R = 2$ are shown in Figure (5.7). In the case shown, the boundary layer is not reached.

4.2.2. Problems without closed form solution for λ_d . In the previous section, the tracking objectives led to stable ODEs for λ_d whose particular solution could be found in closed form. In this section, we consider problems in which this is not the case.

By integrating numerically and simultaneously both the state Equations (2.1) and the ordinary differential equation for the desired flat output λ_d , tracking can be achieved. It is important to notice that realizable objectives imply stable solutions for λ_d . The tracking error dynamics, set by Equation (4.4), makes the flat output in Equation (3.15) converge to the steady state value of λ_d . Tracking is achieved once the transient for both the real and the desired flat outputs vanish.

Due to the non-linear character of the equation for λ_d , the steady state response might exhibit dependence to the initial conditions. For this reason, the control design must start by searching for the initial conditions in λ_d and its derivatives that lead to steady state trajectories that satisfy the desired response specifications. The reader must notice that a fixed number of derivatives of λ_d , three in this case, are needed to build v . This can be obtained by performing additional differentiations on the ODE for λ_d .

As an example, we use the energy-like expression $h(\mathbf{x}, t) = x^2 + y^2 + mz - E(t)$. The corresponding

differential equation for λ_d is given by:

$$\begin{aligned}
0 = & -2E\beta\gamma^2\sigma^2(\dot{\lambda}_d + \lambda_d\beta - k) + 2m\gamma\sigma\beta\dot{\lambda}_d^2 - 4mk\gamma\sigma^2\dot{\lambda}_d + 4m\gamma\sigma^2\beta\lambda_d\dot{\lambda}_d + \\
& 4m\gamma\sigma^2\beta^2\lambda_d^2 + 4mk^2\gamma\sigma^2 + 2m\gamma\sigma\beta^2\lambda_d\dot{\lambda}_d - 2m\gamma\sigma\beta k\dot{\lambda}_d - 8m\gamma\sigma^2\beta k\lambda_d + \\
& 24\beta^2k^2\sigma^2\lambda_d - 24\sigma^2\beta k\dot{\lambda}_d^2 + 24k^2\sigma^2\beta\dot{\lambda}_d - 48\sigma^2k\beta^2\lambda_d\dot{\lambda}_d + 8\sigma^2\beta\dot{\lambda}_d^3 - \\
& 8k^3\sigma^2\beta + 4\beta^3\gamma\sigma^2\lambda_d^2 + \gamma\beta\ddot{\lambda}_d^2 + 2\gamma\beta^2\dot{\lambda}_d\ddot{\lambda}_d + 4\gamma\sigma\beta\ddot{\lambda}_d\dot{\lambda}_d + 4\gamma\sigma\beta^3\lambda_d\dot{\lambda}_d - \\
& 8k\gamma\sigma^2\beta\dot{\lambda}_d + 4\gamma\sigma\beta^2\dot{\lambda}_d^2 + 4k^2\gamma\sigma^2\beta - 4k\gamma\sigma\beta\ddot{\lambda}_d - 4k\gamma\sigma\beta^2\dot{\lambda}_d + 8\gamma\sigma^2\beta^2\lambda_d\dot{\lambda}_d + \\
& 4\gamma\sigma^2\beta\dot{\lambda}_d^2 - 8\beta^2k\gamma\sigma^2\lambda_d + 4\gamma\sigma\beta^2\lambda_d\ddot{\lambda}_d + \gamma\beta^3\dot{\lambda}_d^2 + 8\beta^4\sigma^2\lambda_d^3 + 24\beta^3\sigma^2\lambda_d^2\dot{\lambda}_d - \\
& 24\beta^3\sigma^2k\lambda_d^2 + 24\sigma^2\beta^2\lambda_d\dot{\lambda}_d^2
\end{aligned} \tag{4.7}$$

The set of equations to be integrated numerically is given by Equations (2.1) and (4.7), where u is given by Equations (4.1) and (4.4). The reader must notice that λ_d does not depend on the states and that both equations are coupled via u . Numerical simulations with $E(t) = a + b\sin(\omega t)\cos(\omega t)$ are shown in Figure (5.8).

5. Conclusions. This paper studies the stabilization and tracking control of the Lorenz system using feedback linearization and differential flatness. When the Rayleigh number is used as the control variable, the system is uncontrollable in a manifold of the state space. In the vicinity of such a singularity, the control demands grow unbounded. Composite controllers that use feedback linearization and the system response to step inputs are proposed to overcome this difficulty. By inducing the chaotic response within a boundary layer which contains the singular plane, the transition to desired states is achieved. Such controls can be used not only to enlarge the controllability region of the system to the whole state space but also to mitigate high control demands. Control objectives and initial conditions that imply single and multiple crossings of the boundary layer are studied in the examples. In addition, tracking control problems that involve single and cooperative relations among the states are studied using the differential flatness of the system. Problems with control objectives that lead to integrable and non-integrable differential equations for the desired flat output are considered. A numerical approach in which the state equations and the differential equation for the nominal flat output are simultaneously integrated is proposed and validated. Numerical simulations led to excellent performances.

Acknowledgments. The author would like to thank Professor Sunil K. Agrawal from University of Delaware for his feedback and enthusiasm.

REFERENCES

- [1] J. ALVAREZ-GALLEGOS, *Nonlinear regulation of a Lorenz system by feedback linearization techniques*, Dynamics and Control, 4 (1994), pp. 277–298.
- [2] L. CHEN AND Y. LIU, *Control of the Lorenz chaos by the exact linearization*, Applied Mathematics and Mechanics, 19 (1998), pp. 67–73.
- [3] L. G. CRESPO AND J. Q. SUN, *Feedback linearization of the lorenz system: Stabilization and tracking*, Submitted to the Journal of Vibration and Control, (2002).
- [4] M. FLIESS, J. LEVINE, P. MARTIN, AND P. ROUCHON, *Flatness and defect of non-linear systems: Introductory theory and examples*, International Journal of Control, 61 (1995), pp. 1327–1361.

- [5] F. GAO, W. Q. LIU, V. SREERAM, AND K. L. TEO, *Nonlinear feedback control for the Lorenz system*, Dynamics and Control, 11 (2001), pp. 57–69.
- [6] A. ISIDORI, *Nonlinear Control Systems*, Springer-Verlag, New York, 1989.
- [7] H. SIRA-RAMIREZ, R. CASTRO, AND E. LICEAGA, *Liouvillian systems approach for the trajectory planning-based control of helicopter models*, International Journal of Robust and Non-linear Control, 10 (2000), pp. 301–320.
- [8] C. SPARROW, *The Lorenz Equations: Bifurcations, Chaos and Strange Attractors*, Springer-Verlag, New York, 1982.
- [9] S. TALWAR AND N. S. NAMACHCHIVAYA, *Control of chaotic systems: Applications to the Lorenz equations*, Proceedings of Nonlinear Vibrations, ASME, 50 (1992).
- [10] T. L. VINCENT AND J. YU, *Control of a chaotic system*, Dynamics and Control, 1 (1991), pp. 35–52.

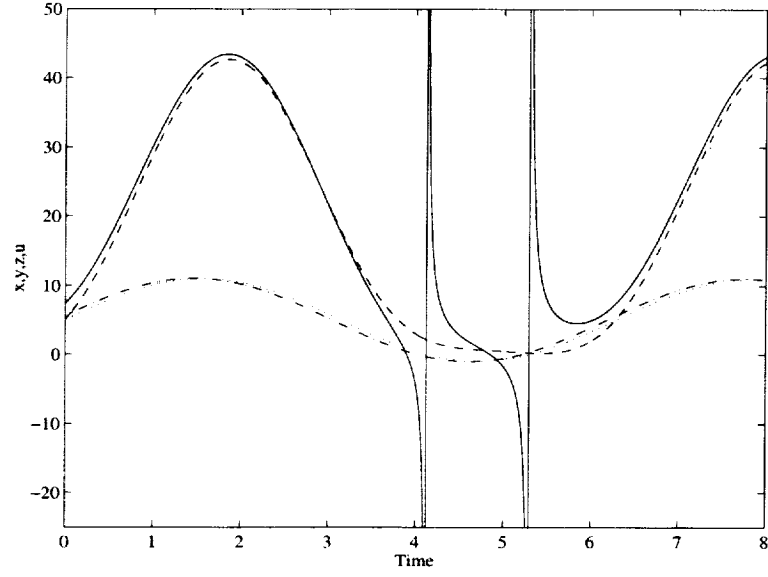


FIG. 5.1. Nominal time histories of u (solid line), x (dot-dashed line), y (dotted line), and z (dashed line) when the reference trajectory is $x_d(t) = 5 + 6\sin(\omega t)$.

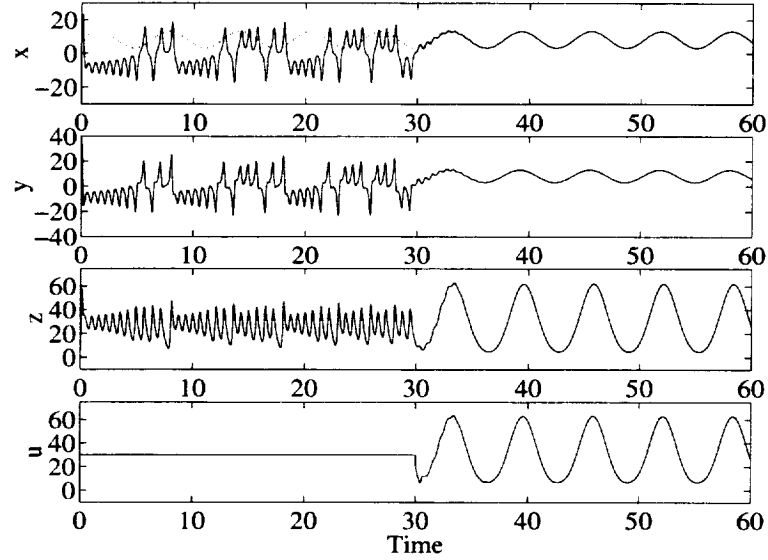


FIG. 5.2. Time evolutions of the state variables and the control with $\delta = 0.1$, $a = 8$ and $b = 5$. The control is activated after 30s. The system does not reach the boundary layer.

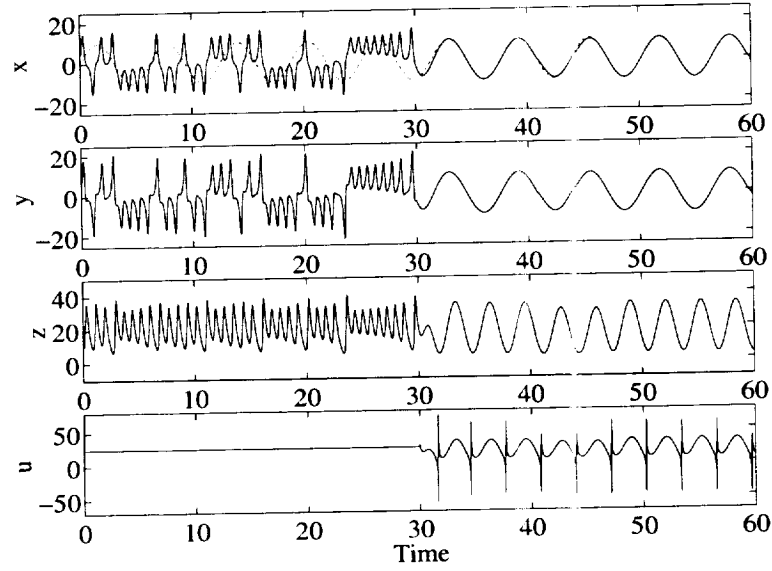


FIG. 5.3. Time evolutions of the state variables and the control with $\delta = 0.2$, $a = 0$ and $b = 10$. The control is activated after 30s. Sharp peaks in the control curve indicate that the system reaches the singularity.

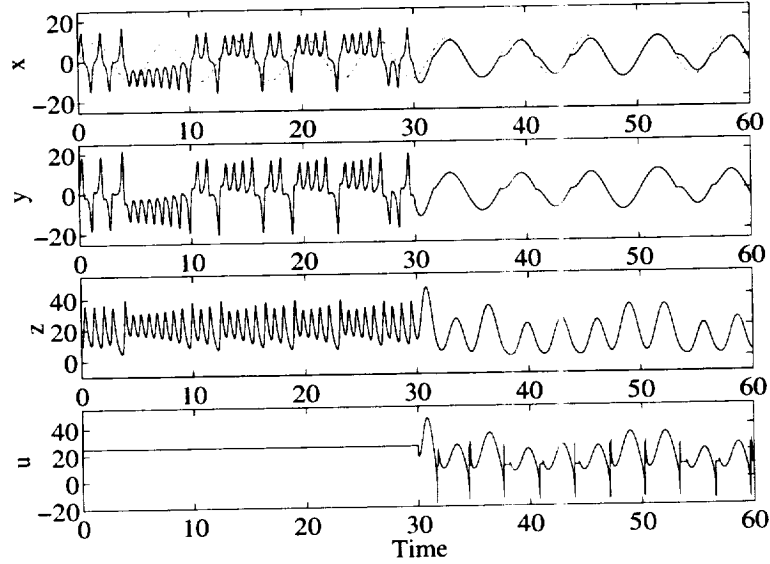


FIG. 5.4. Time evolutions of the state variables and control with $\delta = 0.5$, $a = 0$ and $b = 10$. The control is activated after 30s. Sharp peaks in the control curve indicate that the system reaches the singularity.

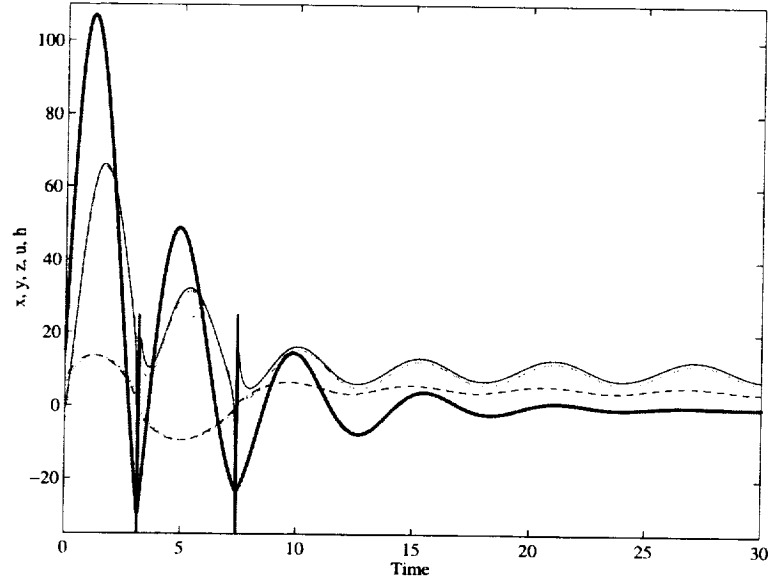


FIG. 5.5. Time evolutions of the state variables and the control for tracking the hyper-plane $h(\mathbf{x}, t) = x^2 - z - 15 - 5 \sin(\omega t)$. The following conventions are used x (dotted line), y (dot-dashed line), z (dashed line), u (solid line) and h (thick line)

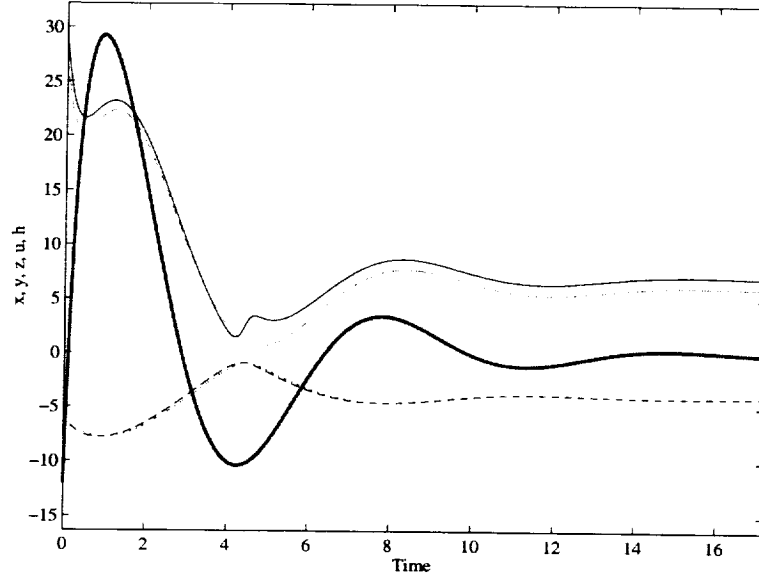


FIG. 5.6. Time evolutions of the state variables and the control for tracking the hyper-plane $h(\mathbf{x}) = x^2 - z - 10$. The following conventions are used x (dotted line), y (dot-dashed line), z (dashed line), u (solid line) and h (thick line).

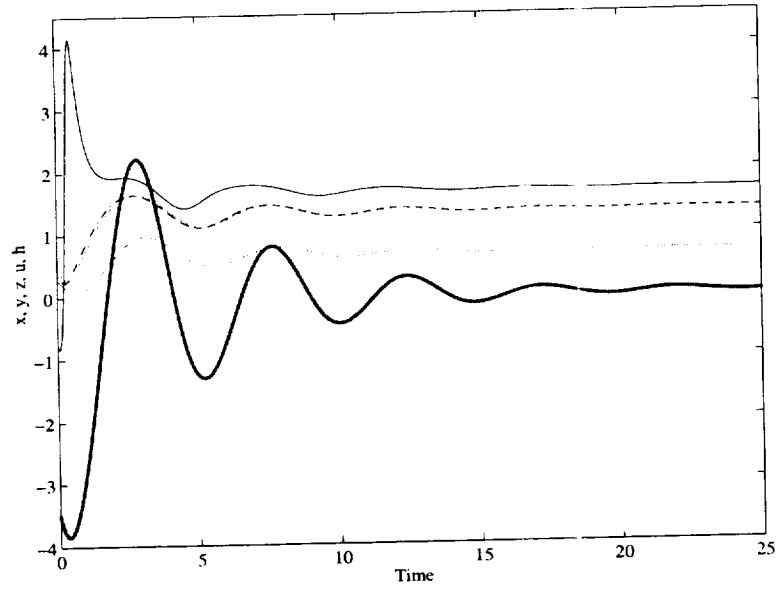


FIG. 5.7. Time evolutions of the state variables and the control for tracking the hyper-plane $h(\mathbf{x}) = x^2 + y^2 + z^2 - 4$. The following conventions are used x (dotted line), y (dot-dashed line), z (dashed line), u (solid line), and h (thick line)

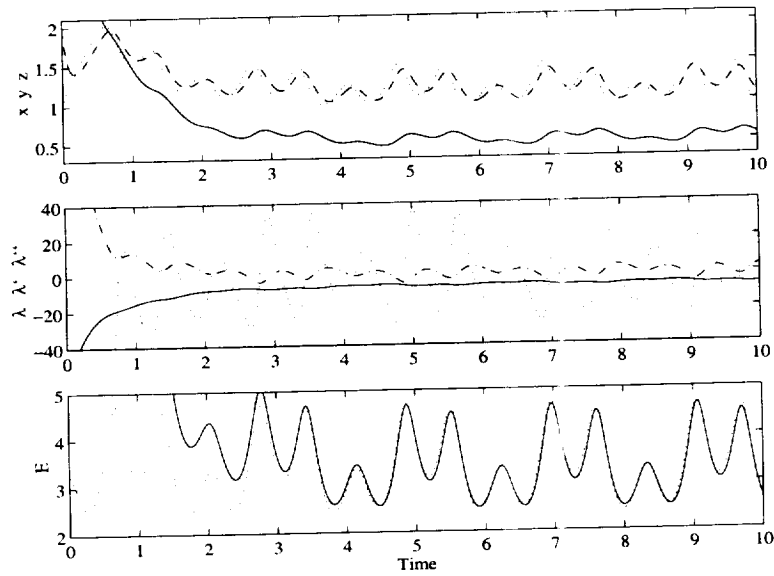


FIG. 5.8. On the top, time evolutions of the states x (dotted line), y (dashed line) and z (solid line) are shown. In the middle, time evolutions for the flat output and its derivatives are shown. In the bottom, time evolutions of $E(t)$ for both, the desired (solid line) and the real (dotted line) flat outputs are shown.

REPORT DOCUMENTATION PAGE			Form Approved OMB No. 0704-0188	
Public reporting burden for this collection of information is estimated to average 1 hour per response, including the time for reviewing instructions, searching existing data sources, gathering and maintaining the data needed, and completing and reviewing the collection of information. Send comments regarding this burden estimate or any other aspect of this collection of information, including suggestions for reducing this burden, to Washington Headquarters Services, Directorate for Information Operations and Reports, 1215 Jefferson Davis Highway, Suite 1204, Arlington, VA 22202-4302, and to the Office of Management and Budget, Paperwork Reduction Project (0704-0188), Washington, DC 20503.				
1. AGENCY USE ONLY(Leave blank)	2. REPORT DATE October 2002	3. REPORT TYPE AND DATES COVERED Contractor Report		
4. TITLE AND SUBTITLE DIFFERENTIAL FLATNESS AND COOPERATIVE TRACKING IN THE LORENZ SYSTEM		5. FUNDING NUMBERS C NAS1-97046 WU 505-90-52-01		
6. AUTHOR(S) Luis G. Crespo				
7. PERFORMING ORGANIZATION NAME(S) AND ADDRESS(ES) ICASE Mail Stop 132C NASA Langley Research Center Hampton, VA 23681-2199		8. PERFORMING ORGANIZATION REPORT NUMBER ICASE Report No. 2002-32		
9. SPONSORING/MONITORING AGENCY NAME(S) AND ADDRESS(ES) National Aeronautics and Space Administration Langley Research Center Hampton, VA 23681-2199		10. SPONSORING/MONITORING AGENCY REPORT NUMBER NASA/CR-2002-211920 ICASE Report No. 2002-32		
11. SUPPLEMENTARY NOTES Langley Technical Monitor: Dennis M. Bushnell Final Report To be submitted to the American Control Conference, 2003.				
12a. DISTRIBUTION/AVAILABILITY STATEMENT Unclassified-Unlimited Subject Category 64 Distribution: Nonstandard Availability: NASA-CASI (301) 621-0390		12b. DISTRIBUTION CODE		
13. ABSTRACT (Maximum 200 words) In this paper the control of the Lorenz system for both stabilization and tracking problems is studied via feedback linearization and differential flatness. By using the Rayleigh number as the control -only variable physically tunable- a barrier in the controllability of the system is incidentally imposed. This is reflected in the appearance of a singularity in the state transformation. Composite controllers that overcome this difficulty are designed and evaluated. The transition through the manifold defined by such a singularity is achieved by inducing a chaotic response within a boundary layer that contains it. Outside this region, a conventional feedback nonlinear control is applied. In this fashion, the authority of the control is enlarged to the whole state space and the need for high control efforts is mitigated. In addition, the differential parametrization of the problem is used to track nonlinear functions of one state variable (single tracking) as well as several state variables (cooperative tracking). Control tasks that lead to integrable and non-integrable differential equations for the nominal flat output in steady-state are considered. In particular, a novel numerical strategy to deal with the non-integrable case is proposed. Numerical results validate very well the control design.				
14. SUBJECT TERMS feedback linearization, differential flatness, Lorenz system, cooperative tracking, non-linear control		15. NUMBER OF PAGES 18		
		16. PRICE CODE A03		
17. SECURITY CLASSIFICATION OF REPORT Unclassified	18. SECURITY CLASSIFICATION OF THIS PAGE Unclassified	19. SECURITY CLASSIFICATION OF ABSTRACT	20. LIMITATION OF ABSTRACT	